arXiv:1611.08939v1 [physics.ins-det] 28 Nov 2016

Higher Order Reentrant Post Modes in Cylindrical Cavities

Ben T. McAllister,[1, a)] Yifan Shen,[2] Stephen R. Parker,[1] and Michael E. Tobar[1, b)]
[1)] *ARC Centre of Excellence for Engineered Quantum Systems, School of Physics, The University of Western Australia, 35 Stirling Highway, Crawley 6009, Western Australia, Australia*
[2)] *Kuang Yaming Honors School, Nanjing University, 22 Hankou Rd, Gulou Qu, Nanjing Shi, Jiangsu Sheng, China, 210000*

(Dated: 29 November 2016)

Reentrant cavities are microwave resonant devices employed in a number of different areas of physics. They are appealing due to their simple frequency tuning mechanism, which offers large tuning ranges. Reentrant cavities are, in essence, 3D lumped LC circuits consisting of a conducting central post embedded in a resonant cavity. The lowest order reentrant mode (which transforms from the TM_{010} mode) has been extensively studied in past publications. In this work we show the existence of higher order reentrant post modes (which transform from the TM_{01n} mode family). We characterize these new modes in terms of their frequency tuning, filling factors and quality factors, as well as discuss some possible applications of these modes in fundamental physics tests.

I. INTRODUCTION

The cylindrical reentrant cavity is a device that can provide high-Q microwave modes with large tuning ranges. It consists of a metal cavity with a conducting post or ring located centrally within the cavity. The gap between the top of this post or ring and the top of the cavity adjusts the mode frequency and at certain gap spacings traps the electric field within the gap. Such cavity designs have been extensively studied and allow for a standard reentrant mode tuning range on the order of GHz without the need for physically large cavities.[1–6]

Since this structure was first investigated in connection with the development of klystrons, it has been widely used in the construction of microwave oscillators and particle accelerators[7,8], and is often chosen as a structure in the study of metamaterials[9,10]. Some recent work has discussed potential applications in telecommunications[11], and detection of gravitational waves[12,13] and dark matter[14]. It is an interesting perspective to view the standard reentrant mode as a perturbed TM_{010} mode. The standard reentrant mode transforms into the empty cavity TM_{010} mode as the central post is removed from the cavity[15]. In a similar way, there exist higher order reentrant modes, which can be viewed as perturbed TM_{01n} modes.

In this work we unequivocally demonstrate the existence of these higher order reentrant modes and characterize them in terms of their tuning range, and quality factor. Section II presents a theoretical study of these modes based on finite element analysis, and experimental data follows in Section III. Finally, these results are summarized and concluded in Section IV.

II. FINITE ELEMENT ANALYSIS OF THE REENTRANT CAVITY

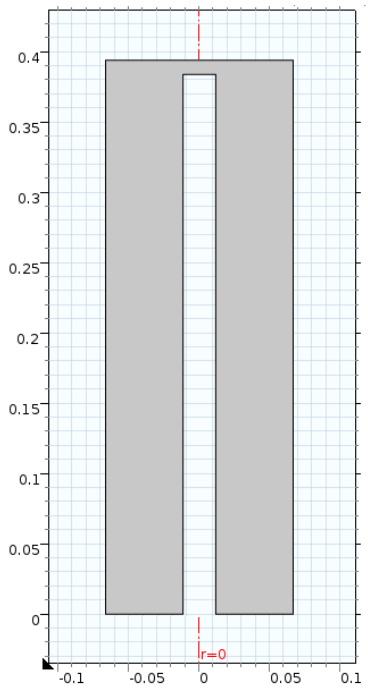

FIG. 1: Cylindrical cross-section of the cavity from the COMSOL model in the r-z plane (encompassing the origin) in cylindrical coordinates. Grey represents the empty cavity space, while the metallic cavity region is represented by grid-lined white area. The height of cavity is ∼0.4 m and the diameter of the inner wall is 0.1337 m. The diameter of the central post is 0.024 m. The gap changes from 0.0001 m to 0.4 m in the simulation.

[a)] Electronic mail: ben.mcallister@uwa.edu.au
[b)] Electronic mail: michael.tobar@uwa.edu.au

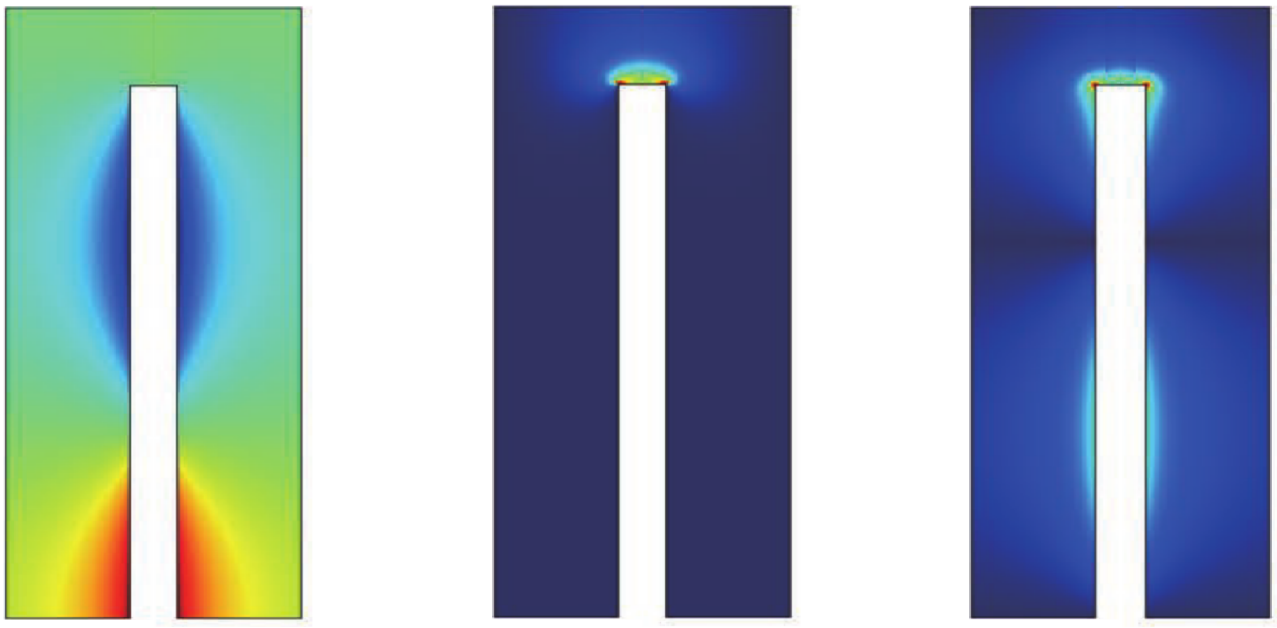

FIG. 2: B_ϕ, E_z and E_r field components for the first higher order reentrant mode are shown from left to right, with a gap size of 5 cm.

We employed the COMSOL Multiphysics software to simulate a reentrant cavity structure. Since the single post reentrant cavity is an axisymmetric structure, it sufficed to use 2D modelling, with revolution around the z-axis. The structure of interest is shown in fig. 1.

We find that multiple higher order modes in the single post reentrant cavity follow similar mode structures to the standard reentrant mode. All of the these modes have the same dominant field components: the axial electric field, E_z, which is located in the region directly above the post and below the top of the cavity, the azimuthal magnetic field B_ϕ, which is separated into several rings surrounding the central post, in alternating phase, and a radial electric field, E_r, due to the gradient of B_ϕ in the z direction. Fig. 2 shows the features of these modes.

The main feature of interest in the higher order modes is the azimuthal magnetic field, which alternates in direction between clockwise and counter-clockwise around the post. We name these higher order modes by their axial wave number, or the number of these "magnetic rings" minus one. Unlike the standard reentrant mode, the higher order modes store their electric energy both in the gap region and cylinder region. The former is determined by the strong E_z field in the central post gap region, and the latter is determined by the radial electric field in the cylinder region which is strongest at the nodes of magnetic field between the "magnetic rings".

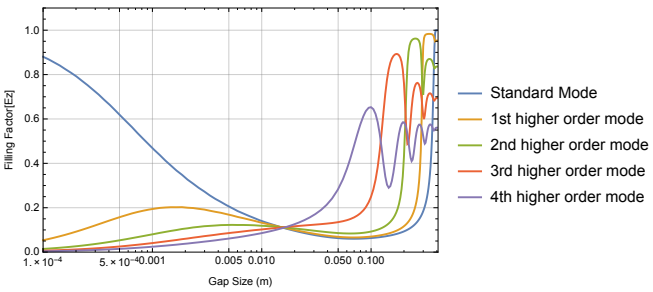

FIG. 3: E_z filling factors for multiple reentrant modes as a function of gap size.

Because of the existence of a radial electric field, higher order mode filling factors differ from the standard reentrant mode. This can be readily observed when the size of the gap becomes very small. Fig. 3 shows the E_z filling factor of different modes, defined as

$$FF = \frac{\int dV\,|E_z|^2}{\int dV\,|E_c|^2}. \tag{1}$$

Where E_c is the electric field in the cavity. When the gap is of the order of mm, the capacitance of the structure formed by the two planes (the top of the post and the top of the cavity) becomes large, and the electric field in this area becomes stronger. In the standard reentrant mode, without other components of electric field outside the gap region, the E_z filling factor approaches unity. However, because the filling factor is related to the integration volume, and due to the existence of radial electric field components in the larger non-gap region, the Ez filling factors of higher order modes may first increase as the gap decreases but eventually approaches zero when the volume of the gap region becomes small.

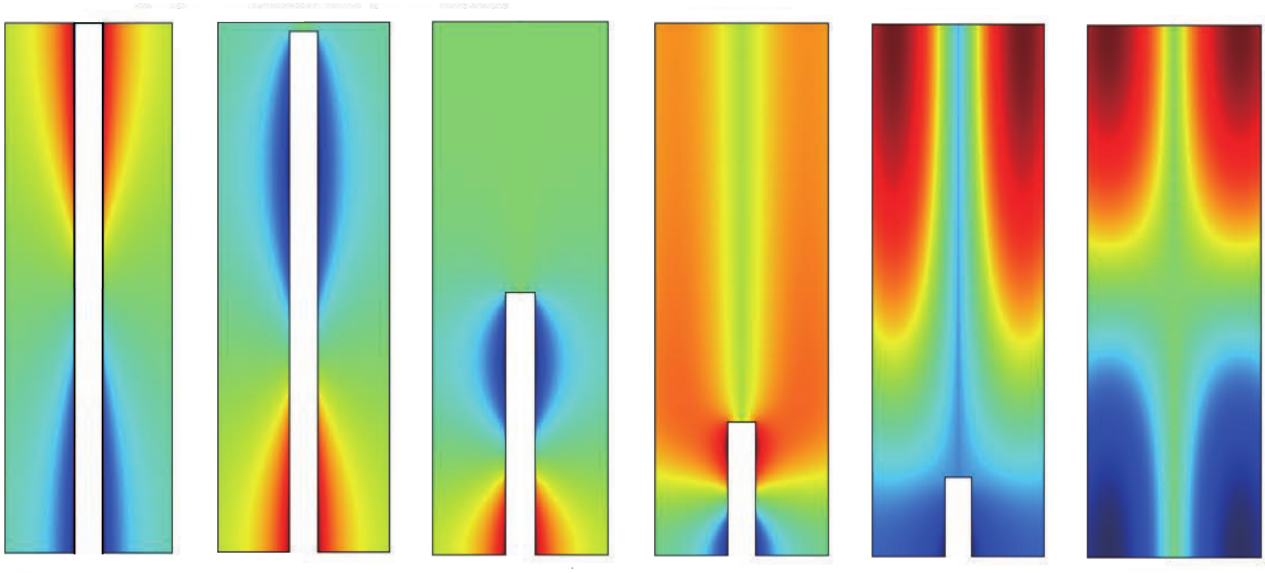

FIG. 4: B_ϕ component transformation of the 1st higher order reentrant mode. From left to right: the first image represents the corresponding coaxial mode, the second and third images represent the purely reentrant mode. The fourth image shows the transition from the reentrant phase to the 'psuedo-TM' phase. The fifth image shows the 'pseudo-TM' phase of the 1st higher order mode. The sixth image shows the TM_{011} mode in the cylindrical cavity. Redder regions represent regions of higher positively signed magnetic field, whilst bluer regions represent regions of higher negatively signed magnetic field.

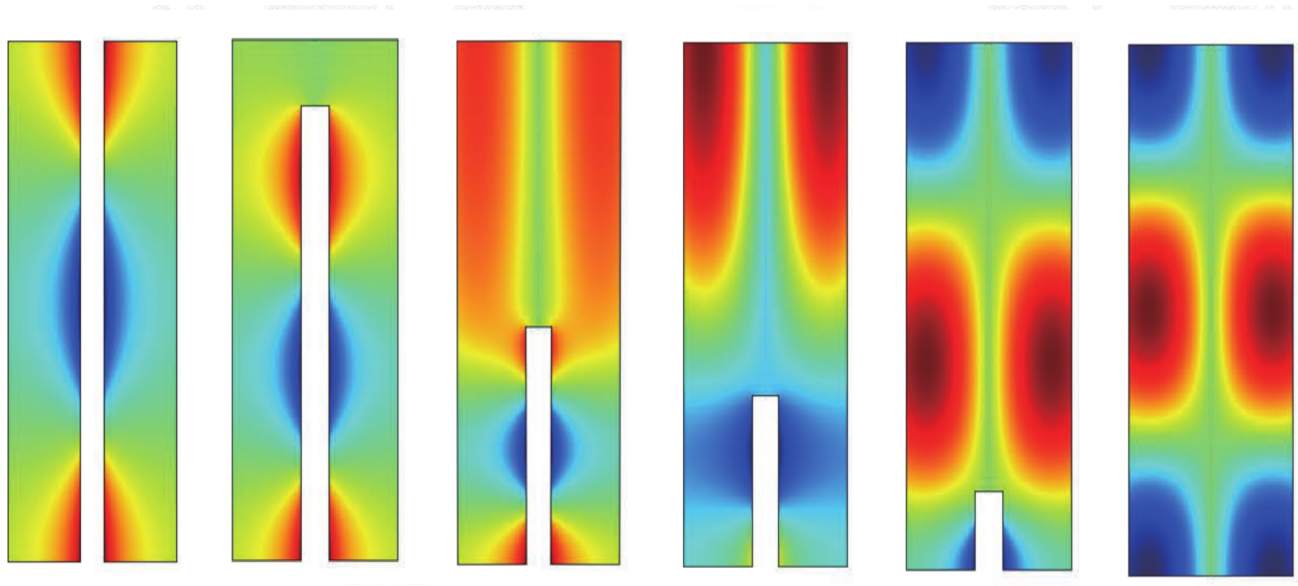

FIG. 5: B_ϕ component transformation of the 2nd higher order reentrant mode. From left to right: the first image represents the corresponding coaxial mode, the second image represents the purely reentrant mode. The third image shows the transition from the reentrant phase to the 'psuedo-TM' phase. The fourth and fifth images show the 'pseudo-TM' phase of the 2nd higher order mode, where some of the "magnetic rings" have moved from the post to the cavity. The sixth image shows the TM_{012} mode in the cylindrical cavity. Redder regions represent regions of higher positively signed magnetic field, whilst bluer regions represent regions of higher negatively signed magnetic field.

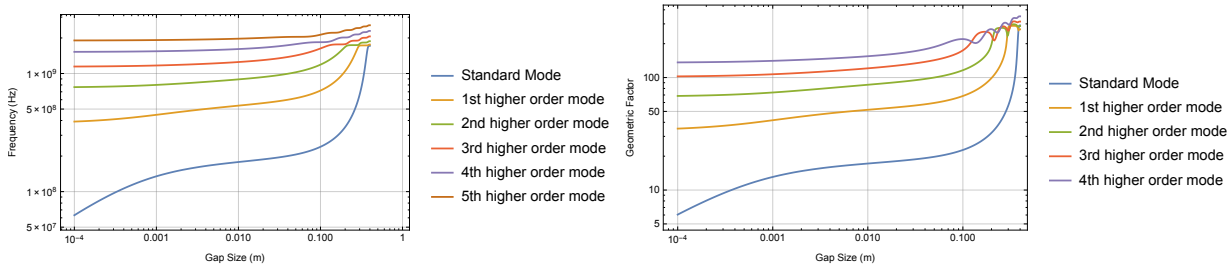

(a) Frequencies of multiple reentrant modes as a function of gap size.

(b) Geometry factors of multiple reentrant modes as a function of gap size.

FIG. 6

Frequency (GHz)	Standard Mode	1st higher order mode	2nd higher order mode	3rd higher order mode	4th higher order mode
Initial	0	0.381	0.761	1.140	1.520
Final	1.72	1.71	1.73	1.73	1.84
Tuning	1.72	1.33	0.967	0.584	0.313

TABLE I: Tuning data for several reentrant modes. The initial frequencies are the frequencies of the modes when the gap size is zero (coaxial regime) where as the final frequencies are the mode frequencies at the end of each modes large tuning phase, when they begin to transition to an empty cavity mode.

Each higher order mode is slightly different, the first higher order mode reaches a maximum E_z filing factor (about 0.2) when the gap is around 0.0015m, yet other modes' E_z filling factors continually decrease as the gap becomes smaller. Unlike the standard reentrant mode, these higher order mode frequencies do not tend to zero as the gap size tends to zero, as their effective capacitance does not tend to infinity due again to the existence of radial electric field components. These modes transition to coaxial modes of fixed frequency when the gap size becomes zero[16].

A common use of a reentrant cavity structure is to utilize the transformation process from empty cavity modes to reentrant modes in order to achieve high frequency tuning ranges. We find that then nth order reentrant mode arises from the transition of a TM01n mode in an empty cylindrical cavity.

Figs. 4 and 5 show the transformation process of the 1st and 2nd higher order modes. As we can see in the figures, because TM_{011} and TM_{012} exhibit periodic change in ϕ direction magnetic field, the transformation process is complex. As the post moves out of the cavity the top "magnetic ring" will transform into the upper lobe of the TM_{01n} empty cylinder mode. As the post continues to move the other rings do the same. The higher order modes undergoes multiple transition phases, from coaxial to reentrant, and from reentrant to empty cylinder via a 'pseudo-TM' phase where some of the "magnetic rings" have become empty cavity lobes. Each mode transitions slightly differently, due to the number of "magnetic rings" and lobes in the empty cavity mode. These transition phases affect frequency tuning.

We have calculated the resonant mode properties as the gap size changes from 0.1mm to ∼40 cm. Fig 6a shows the eigenfrequencies of different reentrant modes. Table I lists tuning ranges of the standard reentrant mode and some high order modes first phases. As mentioned, higher order modes go through multiple phases, with the first phase, the purely reentrant phase, exhibiting the largest tuning range. After this point the modes become quite crowded in frequency space, as they are nearly at the frequencies of the corresponding empty cavity TM modes. By monitoring different modes, it is possible tune through different frequency ranges at the same time, which would be beneficial in many fundamental physics tests such as searches for dark matter and gravitational waves.

We have also characterized these modes in terms of their geometry factor, which is directly proportional to mode quality factor

$$G = \frac{\omega\mu_0 \int \left|\vec{H}\right|^2 dV_c}{\int \left|\vec{H}\right|^2 dS_c} = Q \times R_s. \tag{2}$$

Where R_s is the surface resistivity of the metal. Fig. 6b shows the geometry factors as a function of gap size for various reentrant modes. It is obvious that the geometric factor of higher order modes is much higher than that of the standard mode. High-Q modes are highly sought after in fundamental physics tests[12–14], which makes these modes promising candidates.

FIG. 7: Cavity used for the experiment.

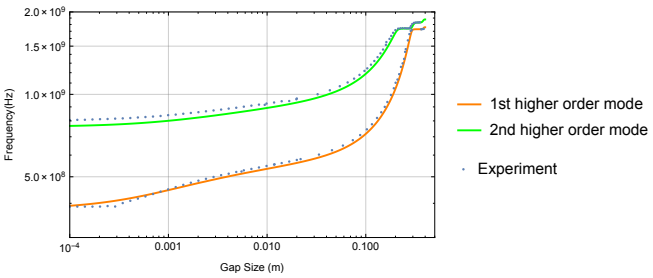

FIG. 8: Experimental and theoretical frequency data of 1st and 2nd higher order reentrant modes. The average error is below 3%.

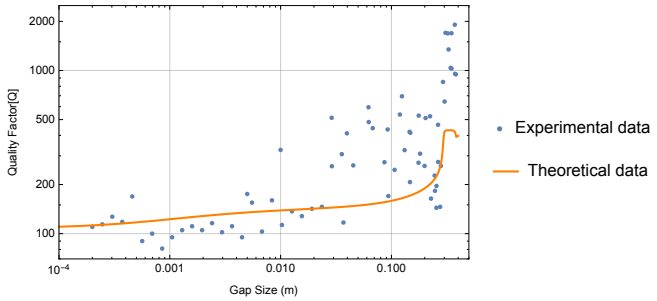

FIG. 9: Quality factor of the 1st higher order reentrant mode as a function of gap size. The experimental data comes from the transmission signal S12. The theoretical data is based on an assumed electrical conductivity of 1.5×10^4 S/m.

III. EXPERIMENTAL DATA

The properties of the resonant modes were measured with a vector network analyzer to acquire the complex value of S21 in transmission[17]. Two loop probes were used for the measurement. One probe was located near the base of the central post through a 1-mm-diameter hole in the lid of the cavity, whilst the other was inserted through a hole on the side wall. Both of these probes were used to couple to the B_ϕ field component. Fig. 7 is the device used for the measurement, which consists of an empty cylindrical cavity, a conducting central post, and a micrometer for the movement of the post. The setup was used to track the frequency of the 1st and 2nd higher order modes, and the results are displayed in fig. 8. On average, the experimental mode frequencies differed from the theory by less than 3%.

Mode quality factor was also measured. Fig. 9 shows the experimental and theoretical data for the 1st higher order mode. The theoretical data uses the geometry factors derived from the finite element analysis, and an electrical conductivity of 1.5×10^4 S/m, which was found from a fit to the experimental data. This value is considerably lower than the accepted value of electrical conductivity for brass ($\sim 1.6 \times 10^7$ S/m[18]), some potential reasons for this are discussed below. We chose to utilize the fit value for the conductivity in order to demonstrate that although the quality factors are lower than anticipated, they do follow the correct trend, ie the quality factor goes through a sharp increase when gap size is around 0.25m, which fits modelled geometry factors well. Fig. 10 shows the effective surface resistance calculated from the theoretical geometric factor and experimental quality factors according to eq 2. The average effective surface resistance is $\sim$3.81 Ω. It is important to note that this high value of resistance (and low value of conductivity) is only an effective surface resistance, as the losses in this system are not limited by the conducting surface. The main reason for this high effective surface resistance is the small gap between the post and the hole in the cavity lid that the

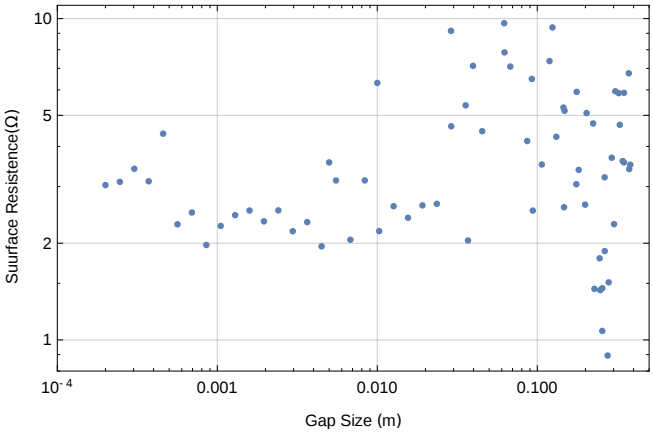

FIG. 10: The effective experimental surface resistivity as a function of gap size.

post slides through. No RF choke was employed where gaps are present as is common in such measurements[19,20]. The post is not directly connected to the cavity in order to allow it to move, this both introduces an extra capacitance and allows considerable radiation leakage, which increases the effective surface resistance. Furthermore, experiments with reentrant cavities in the past have observed discrepancy between experimental and theoretical quality factors[21–23] and attribute this to a number of factors, such as joins between cavity lids and bodies, the existence of probes and probe holes, and loading of the resonance by the external measurement circuit.

IV. SUMMARY AND CONCLUSION

In summary, we have demonstrated the existence of higher order reentrant modes with higher frequencies than the fundamental in the single-post cylrindrical reentrant cavity. We have verified our finite-element modelling by comparison with experimental data, and the agreement is good. We find that the higher order reentrant modes arise from perturbed TM_{01n} modes in empty cylinders, and finally convert to coaxial modes when the gap size becomes zero. The higher order reentrant modes have higher geometry factors when compared to the standard reentrant mode. We have found and characterized the different phases that exist in the transformation process. These modes have possible applications in a number of fundamental physics tests, such as gravity wave and dark matter detection experiments. Furthermore, it is worth considering that an understanding of these reentrant modes affords us a deeper understanding of the highly localized "gap modes" present in many experiments. For example, it has been discussed that axion haloscope experiments utilizing tuning rods to adjust mode frequency can have their sensitivity degraded by the presence of highly localized modes which arise due to the small gap between the end of the tuning rod and the walls of the cavity, which must exist for real tuning rods[24].

ACKNOWLEDGMENTS

This work was supported by Australian Research Council grant CE110001013, as well as the UWA-China Research Training Program, the Australian Postgraduate Award and the Bruce and Betty Green Foundation.

[1] N. C. Carvalho, Y. Fan and M. E. Tobar, arXiv:1603.04848 [physics.ins-det].
[2] M. Goryachev and M. E. Tobar, New J. Phys. **17**, no. 2, 023003 (2015) doi:10.1088/1367-2630/17/2/023003 [arXiv:1408.3228 [physics.ins-det]].
[3] Y. Fan, Z. Zhang, N. C. Carvalho, J.-M. Le Floch, Q. Shan and M. E. Tobar, IEEE Trans. Microwave Theor. Tech. **62**, 1657 (2014) doi:10.1109/TMTT.2014.2331625 [arXiv:1309.7902v3]
[4] M. Jaworski. On the resonant frequency of a reentrant cylindrical cavity. *IEEE Transactions on Microwave Theory and Techniques*, 26(4):256–260, Apr 1978.
[5] K. Fujisawa. General treatment of klystron resonant cavities. *IRE Transactions on Microwave Theory and Techniques*, 6(4):344–358, October 1958.
[6] W. W. Hansen. On the resonant frequency of closed concentric lines. *Journal of Applied Physics*, 10(1), 1939.
[7] A. G. Williamson. The resonant frequency and tuning characteristics of a narrow-gap reentrant cylindrical cavity. *IEEE Transactions on Microwave Theory and Techniques*, 24(4):182–187, Apr 1976.
[8] T. L. Grimm, A. Aizaz, M. Johnson, W. Hartung, F. Marti, D. Meidlinger, M. Meidlinger, J. Popielarski, and R. C. York. New directions in superconducting radio frequency cavities for accelerators. *IEEE Transactions on Applied Superconductivity*, 15(2):2393–2396, June 2005.
[9] Damla Ates, Atilla Ozgur Cakmak, Evrim Colak, Rongkuo Zhao, C. M. Soukoulis, and Ekmel Ozbay. Transmission enhancement through deep subwavelength apertures using connected split ring resonators. *Opt. Express*, 18(4):3952–3966, Feb 2010.
[10] D. R. Smith, Willie J. Padilla, D. C. Vier, S. C. Nemat-Nasser, and S. Schultz. Composite medium with simultaneously negative permeability and permittivity. *Phys. Rev. Lett.*, 84:4184–4187, May 2000.
[11] R. Sorrentino, L. Pelliccia and S. Bastioli, Microwaves, Radar and Remote Sensing Symposium (MRRS) 2011, 20 (2011). doi:10.1109/MRRS.2011.6053593
[12] G. L. Pimentel, O. D. Aguiar, J. J. Barroso and M. E. Tobar, J. Phys. Conf. Ser. **122**, 012028 (2008). doi:10.1088/1742-6596/122/1/012028
[13] V. Liccardo, O. D. Aguiar and E. K. de Frana, arXiv:1511.05902 [astro-ph.IM].
[14] B. T. McAllister, S. R. Parker and M. E. Tobar, Phys. Rev. D **94**, no. 4, 042001 (2016) doi:10.1103/PhysRevD.94.042001 [arXiv:1605.05427 [physics.ins-det]].
[15] J.-M. Le Floch *et al.*, Rev. Sci. Instrum. **84**, 125114 (2013) doi:10.1063/1.4848935 [arXiv:1308.2755 [physics.ins-det]].
[16] H. Wang, K. Wu, J. Litva, IEEE Trans. Microwave Theory Tech. **45**, 414 (1997). doi:10.1109/22.563341
[17] D. Kajfez and E. J. Hwan. Q-factor measurement with network analyzer. *IEEE Transactions on Microwave Theory and Techniques*, 32(7):666–670, Jul 1984.
[18] N. Bowler, Y. Huang, Meas. Sci. Technol. **16**, 2193 (2005). doi:10.1088/0957-0233/16/11/009
[19] B. Xiao, R. L. Geng, C. Reece, F. Marhauser, L. Phillips, H. Wang and M. Kelley, JLAB-ACC-09-981.

[20]P. Goudket *et al.*, doi:10.18429/JACoW-SRF2015-TUPB064
[21]G. Tsanakovam, M. Richter, A. Madigan, P. L. Stanwix, E. F. May, R. Span, J. Chem. Thermodyn. **101**, 395 (2016). doi:10.1016/j.jct.2016.06.005
[22]A. R. H. Goodwin, J. B. Mehl, M. R. Moldover, Rev. Sci. Instrum. **67**, 4294 (1996). doi:10.1063/1.1147580
[23]E. F. May, T. J. Edwards, A. G. Mann, C. Edwards, R. C. Miller, Fluid Phase Equilib. **185**, 339 (2001). doi:10.1016/S0378-3812(01)00482-4
[24]I. Stern, A. A. Chisholm, J. Hoskins, P. Sikivie, N. S. Sullivan, D. B. Tanner, G. Carosi and K. van Bibber, Rev. Sci. Instrum. **86**, no. 12, 123305 (2015) doi:10.1063/1.4938164 [arXiv:1603.06990 [physics.ins-det]].